Journal of the Chinese Institute of Engineers, 2015
Vol. 38, No. 5, 665–674, http://dx.doi.org/10.1080/02533839.2015.1010453

On the simulation of flow around discrete coniferous trees

Fuh-Min Fang*, Tsung-Chi Liang, Cheng-Yang Chung and Yi-Chao Li

Department of Civil Engineering, National Chung Hsing University, 250 Kuo Kuang Road, Taichung 402, Taiwan

(*Received 24 September 2013; accepted 29 April 2014*)

The present study is to establish a numerical model capable of predicting flow past discrete coniferous trees, so as to provide a handy tool for pedestrian wind analysis during the preliminary design stage for local wind environments. In the study, a tree factor was proposed to reflect the effect due to the existence of the trees. Besides the applications of numerical computations in flow analysis, wind tunnel measurements were also performed to guide and confirm the numerical simulations. By comparing the velocity profiles at certain downstream cross-sections of tree panels, the variation of the tree factor was calibrated and the result can be readily used to predict the flow around discrete coniferous trees. Results also showed that the proposed tree factor generally increased with increases in the volume ratio and horizontal thickness of the tree body. Based on the calibrated relationship of the tree factor, finally, additional numerical computations were performed to simulate flow past an isolated tree and dual trees in a tandem and a side-by-side arrangement. The predicted downstream wind velocity profiles appeared in good agreement with the measurement results.

Keywords: Large eddy simulation; wind tunnel test; bluff body aerodynamics

1. Introduction

Planting trees in building areas can not only upgrade the appearance of the local landscape, but, to some extent, also improve the local wind environment, particularly regarding the reduction of wind speed at the pedestrian level. Therefore, how to analyze the wind flow in areas with discrete trees becomes an important task for the designers during the planning stage. Physically, the flow pattern around a tree may appear somewhat different from that around a solid (impermeable) body due to its porous nature. As a portion of wind passes through a tree, the shedding vortices can interact with the associated penetrating flow and disturb the formation of the downstream wake. Intuitively, the extent of this interaction effect can depend on the porosity and thickness of the tree body.

To analyze a flow past discrete trees, wind tunnel model experiments are mostly employed. Besides the amount of human labor and time required in the execution of experimental work being of concern, technical difficulties (such as the scale effect) are generally encountered. In contrast, the adoption of numerical simulations can be another alternative for the flow analysis, as it is considered relatively more economical. Although it is presently impractical to simulate flows around porous trees by taking into account the detailed geometry of leaves and twigs since the work requires a very fine mesh and a great amount of computing time, a second choice may be to find out a factor that physically reflects their existence in the computations.

Accordingly, the goal of this study is to establish a numerical model, capable of predicting flows past discrete trees, so as to provide a handy tool for pedestrian wind analysis during the preliminary design for local wind environments. Particularly, coniferous trees are of concern in this study. Besides numerical computations, wind tunnel measurements were also performed to confirm and guide the numerical simulations.

2. Related studies

Most of the previous related work has concentrated on studies in the research areas of forestry and meteorology. The main focus was to investigate the overall wind flow characteristics around groups of trees in forest territories. Based on a global approach, the three-dimensional (3-D) wind flow analyses were generally simplified into a two-dimensional (2-D) or one-dimensional problem depending on the spatial distributions of local tree groups. Typically, Finnigan (2000) stated that the surface wind flow region could be divided into a canopy and a surface sublayer. By field investigations, Raupach, Antonia, and Rajagopalan (1991) indicated that the pattern of turbulent flow characteristics within the canopy sublayer was close to that of a mixing-layer flow. A description of wind speed profile was also proposed by Raupach,

*Corresponding author. Email: fmfang@nchu.edu.tw

Coppin, and Legg (1986) based on wind tunnel results. Similar profiles in forest territories were also brought out by Mihailovic et al. (1999). Based on wind tunnel results, Massman (1987) proposed a leaf area index and discussed its influence on the associated wind speed profiles, surface shear velocities, and roughness heights. Additionally, Novak et al. (2000) found that a change of the spatial density of trees in a forest could affect the local mean and turbulent flow characteristics, mainly dominated by large-scale turbulence eddies. Further results of wind tunnel experiments by Boldes, Colman and Maranon (2001), regarding wind flows past a single layer and a double layer of plants, revealed that mixing flows occurred in the wake region and produced bleed flows due to the effect of large-scale eddies. Moreover, Flesch and Wilson (1999a, 1999b) carried out wind tunnel experiments to investigate the protected area as well as the extent of wind speed reduction downstream of tree groups.

There are also several studies related to wind flows around trees using numerical analysis. Typically, Shaw and Schumann (1992) proposed an inclusion of a source term in the momentum equations to physically reflect the tree effects. The introduced drag term was the product of the drag coefficient, leaf density, and combined velocity. Wilson and Flesch (1999) used a 2-D numerical model to simulate flows past forests. The predicted wind speed profiles were in good agreement with the in-field results. By performing large eddy simulations, Su et al. (1998) predicted neutrally stratified flows past forests. Patton and Davis (2001) also carried out large eddy simulations to investigate the dispersion mechanism of chemicals in forests. Watanabe (2004) performed large eddy computations to examine the turbulence structure above forests. Moreover, Sladek, Bodnar, and Kozel (2007) investigated numerically the 2- and 3-D wind fields of boundary-layer flows past forests in areas of complex topography.

3. Numerical method

A weakly compressible flow method (Song and Yuan 1988) is adopted in the flow calculations. The original form of the method is applicable to inviscid flow cases and is further extended to viscous turbulent flow simulations. Under a barotropic assumption (density is a function of pressure only) for low Mach number flows, the continuity and momentum equations in index forms can be approximated as (Song and Yuan 1988)

$$\frac{\partial p}{\partial t}+\frac{\partial}{\partial x_j}(Ku_j)=0, \tag{1}$$

$$\frac{\partial u_i}{\partial t}+\frac{\partial u_i u_j}{\partial x_j}=-\frac{1}{\rho}\frac{\partial p}{\partial x_i}+\nu\frac{\partial^2 u_i}{\partial x_j x_j}, \tag{2}$$

where K ($=\rho c^2$) is the bulk modulus of elasticity; ρ, ν, p, u, and c are the density, kinematic viscosity, pressure, velocity, and sound speed, respectively.

For turbulent flows, a large eddy simulation approach is applied. Accordingly, any quantity, g, can be decomposed into resolvable-scale and subgrid-scale components as

$$g=\bar{g}+g'. \tag{3}$$

Through a space-averaging process, the governing equations become

$$\frac{\partial \bar{p}}{\partial t}+\frac{\partial}{\partial x_j}(K\overline{u_j})=0, \tag{4}$$

$$\frac{\partial \bar{u}_i}{\partial t}+\frac{\partial \overline{u_i u_j}}{\partial x_j}=-\frac{\partial(\overline{p/\rho})}{\partial x_i}+\frac{\partial}{\partial x_j}\left[\overline{-u_i'u_j'}-\overline{u_i'\bar{u}_j-\bar{u}_i u_j'}-\left(\overline{\bar{u}_i\bar{u}_j}-\bar{u}_i\bar{u}_j\right)+\nu\frac{\partial \bar{u}_i}{\partial x_j}\right]. \tag{5}$$

By adopting Reynolds' averaging assumption as

$$\overline{u_i'\bar{u}_j-\bar{u}_i u_j'}+\left(\overline{\bar{u}_i\bar{u}_j}-\bar{u}_i\bar{u}_j\right)=0, \tag{6}$$

one obtains

$$\frac{\partial \bar{u}_i}{\partial t}+\frac{\partial \overline{u_i u_j}}{\partial x_j}=-\frac{\partial(\overline{p^*/\rho})}{\partial x_i}+\frac{\partial}{\partial x_j}\left[-\left(\overline{u_i'u_j'}-\frac{1}{3}\overline{u_i'u_j'}\delta_{ij}\right)+\nu\frac{\partial \bar{u}_i}{\partial x_j}\right], \tag{7}$$

where δ_{ij} is the Kronecker delta function and $p^*=p+(\rho/3)\overline{u_i'u_i'}$.

As the subgrid-scale stress terms are modeled by

$$-\left(\overline{u_i'u_j'}-\frac{1}{3}\ \overline{u_i'u_j'}\ \delta_{ij}\right)=\nu_t S_{ij}, \tag{8}$$

where

$$S_{ij}=\left(\frac{\partial \bar{u}_j}{\partial x_i}+\frac{\partial \bar{u}_i}{\partial x_j}\right). \tag{9}$$

Equation (7) becomes

$$\frac{\partial \bar{u}_i}{\partial t}+\frac{\partial \bar{u}_i\bar{u}_j}{\partial x_j}=-\frac{\partial(\overline{p^*/\rho})}{\partial x_i}+\frac{\partial}{\partial x_j}[\tau_{ij}], \tag{10}$$

where τ_{ij} is the combination of the viscous term and the subgrid-scale stress term, in which the subgrid-scale diffusion coefficient is expressed in the form suggested by Smagorinsky (1963) as

$$\nu_t = (C_S\Delta)^2\sqrt{\frac{S_{ij}^2}{2}}, \tag{11}$$

where Δ is the characteristic length of the computational cell and C_S is the Smagorinsky constant.

In the flow computations, a finite-volume approach is employed to obtain the solutions of Equations (7) and (10) for spatial volumes wholly occupied by air. For the computational cells containing leaves and twigs, on the other hand, the momentum equation is modified by adding a source term proposed by Shaw and Schumann (1992) as

$$\frac{\partial \bar{u}_i}{\partial t} + \frac{\partial \bar{u}_i\bar{u}_j}{\partial x_j} = -\frac{\partial(\overline{p^*/\rho})}{\partial x_i} + \frac{\partial}{\partial x_j}[\tau_{ij}] + (\boldsymbol{f_D})_i, \tag{12}$$

with

$$\boldsymbol{f_D} = [-C_D\, a\, u\, \boldsymbol{V}, -C_D\, a\, v\, \boldsymbol{V}, -C_D\, a\, w\, \boldsymbol{V}], \tag{13}$$

where C_D is the drag coefficient and "a" is the leaf surface area per unit volume.

Equations (4) and (10) (or Equation (12)) can be presented in a conservative form as

$$\frac{\partial G}{\partial t} + \nabla \cdot \boldsymbol{F} = 0 \tag{14}$$

The computation can proceed using an integration over a specific control volume ($\forall$) as

$$\int_\forall \frac{\partial G}{\partial t} d\forall + \int_\forall \nabla \cdot \boldsymbol{F}\, d\forall = 0. \tag{15}$$

By the divergence theorem, one has

$$\frac{\partial G_m}{\partial t} = -\int_S \boldsymbol{n} \cdot \boldsymbol{F}\, dS/\forall, \tag{16}$$

where G_m is the mean quantity referred to the center of the volume (computational cell) and $\boldsymbol{n}$ is the normal surface vector. By knowing the G_m quantities of the flow field at a starting time step, the integral form of Equation (16) can be used to calculate the change of G_m within an elapsed period, Δt, to further update the G_m values for the next time step.

In the computations, appropriate pressure and velocity values are specified at exterior phantom cells outside the boundaries to reflect the correct physical nature of the boundaries. For solid boundaries, a no-slip condition is used. At the upstream section, a prescribed velocity profile is imposed. On the other hand, the average pressure at the downstream end section is set as the reference pressure. On the boundary at the top, the values at the phantom cells are specified according to a zero-gradient assumption in the direction normal to the boundary.

4. Wind tunnel experiments

Experiments were conducted at the Architecture and Building Research Institute wind tunnel in Taiwan. The size of the test section is 2.6 m in height and 4.0 m in width. The maximum wind speed in the test section is 35 m/s with a turbulent intensity less than 1%. In the experiments, rectangular panels (D = 0.28 m and B varies from 0.14–0.56 m), containing a number of parallel and evenly spaced coniferous leaf strings (Figure 1), were installed (horizontally) in the direction perpendicular to the uniform approaching flow (see Figure 2; U_o = 10 m/s) at a location near the center of the tunnel cross-section. The shape of the leaves is roughly cylindrical with a diameter of 0.0012 m and a length of 0.035 m on average. The Reynolds number ($Re = U_oD/\nu$; ν is the kinematic viscosity of air) is about 3.83×10^5.

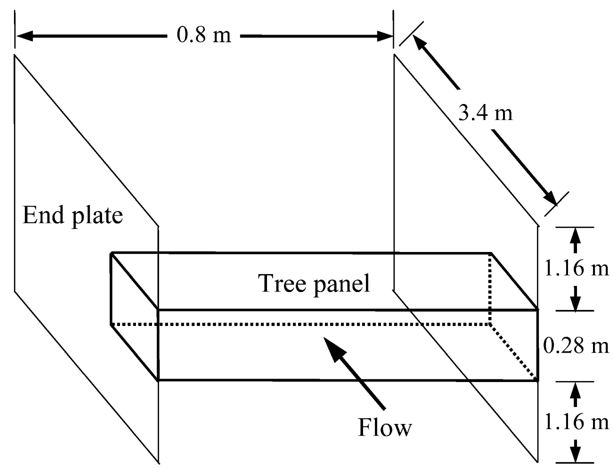

Figure 1. Sketch of experimental setup.

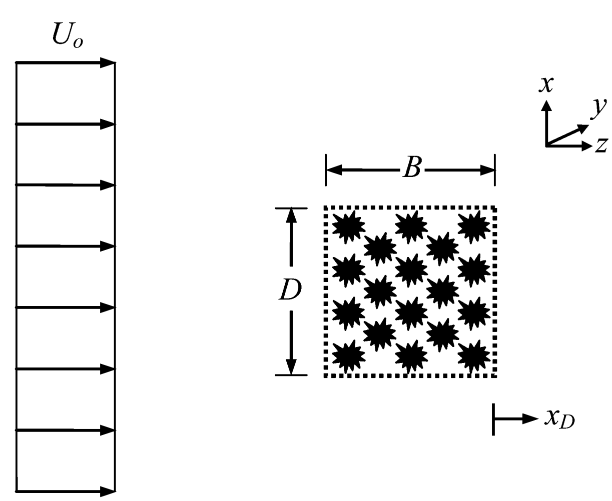

Figure 2. Schematic of wind tunnel experiments.

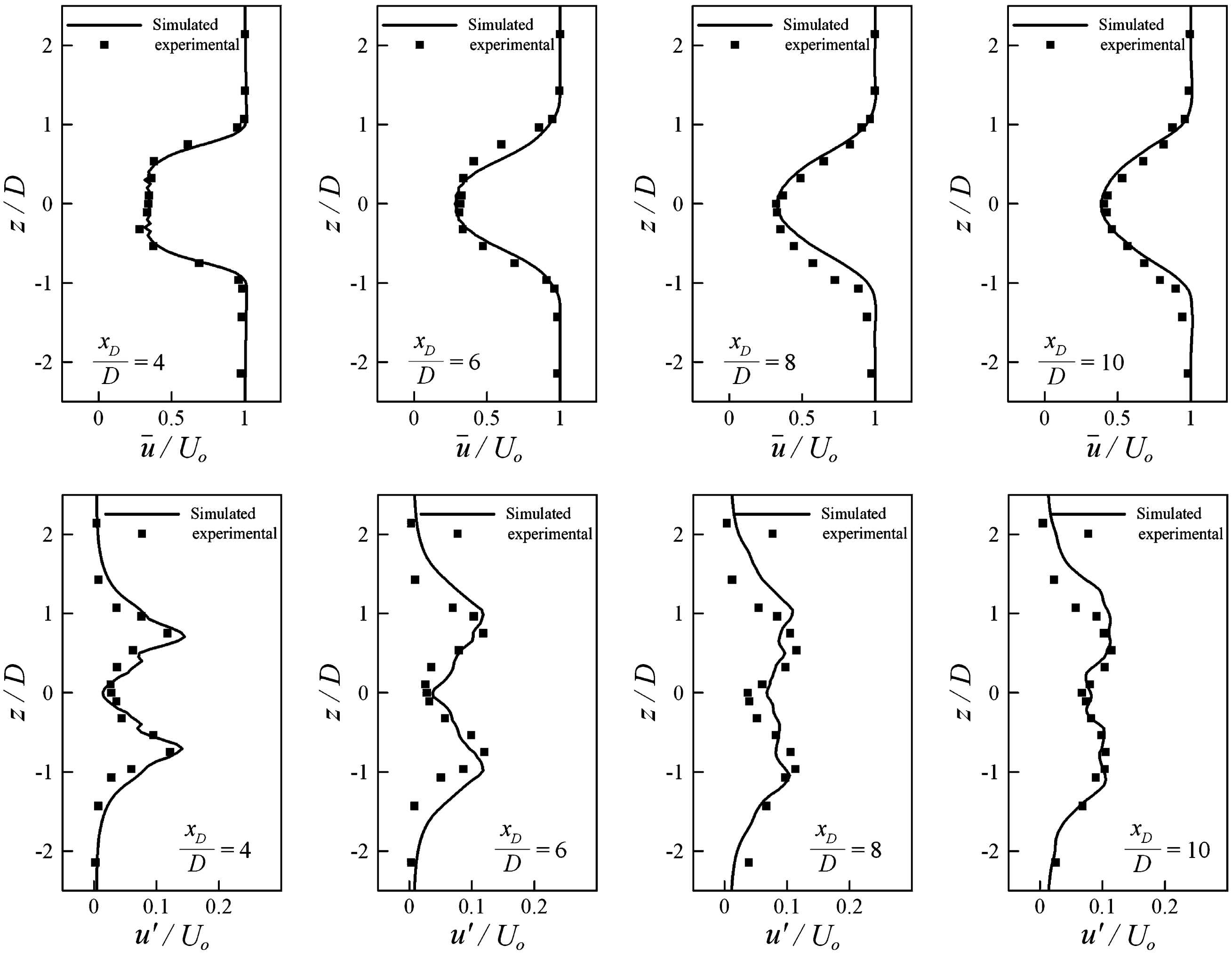

Figure 3. Comparison of mean and rms velocity profiles behind a tree panel.

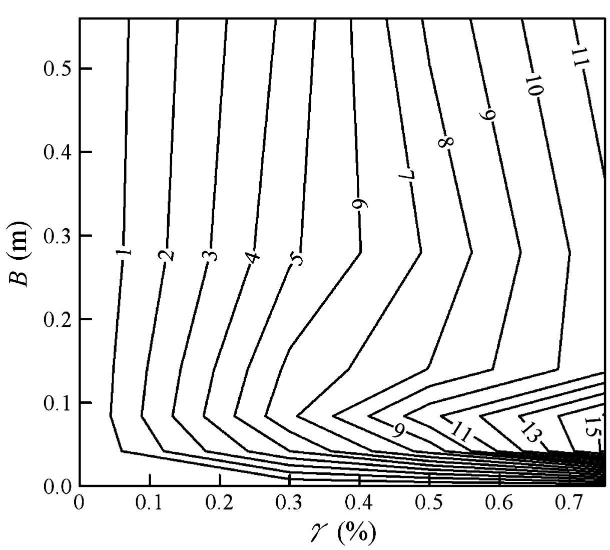

Figure 4. Contours of C_{Da} (in m^{-1}).

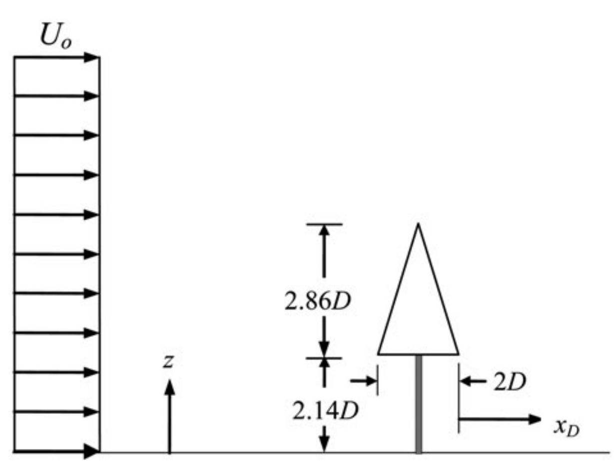

Figure 5. Schematic of flow past an isolated tree body with a conical shape.

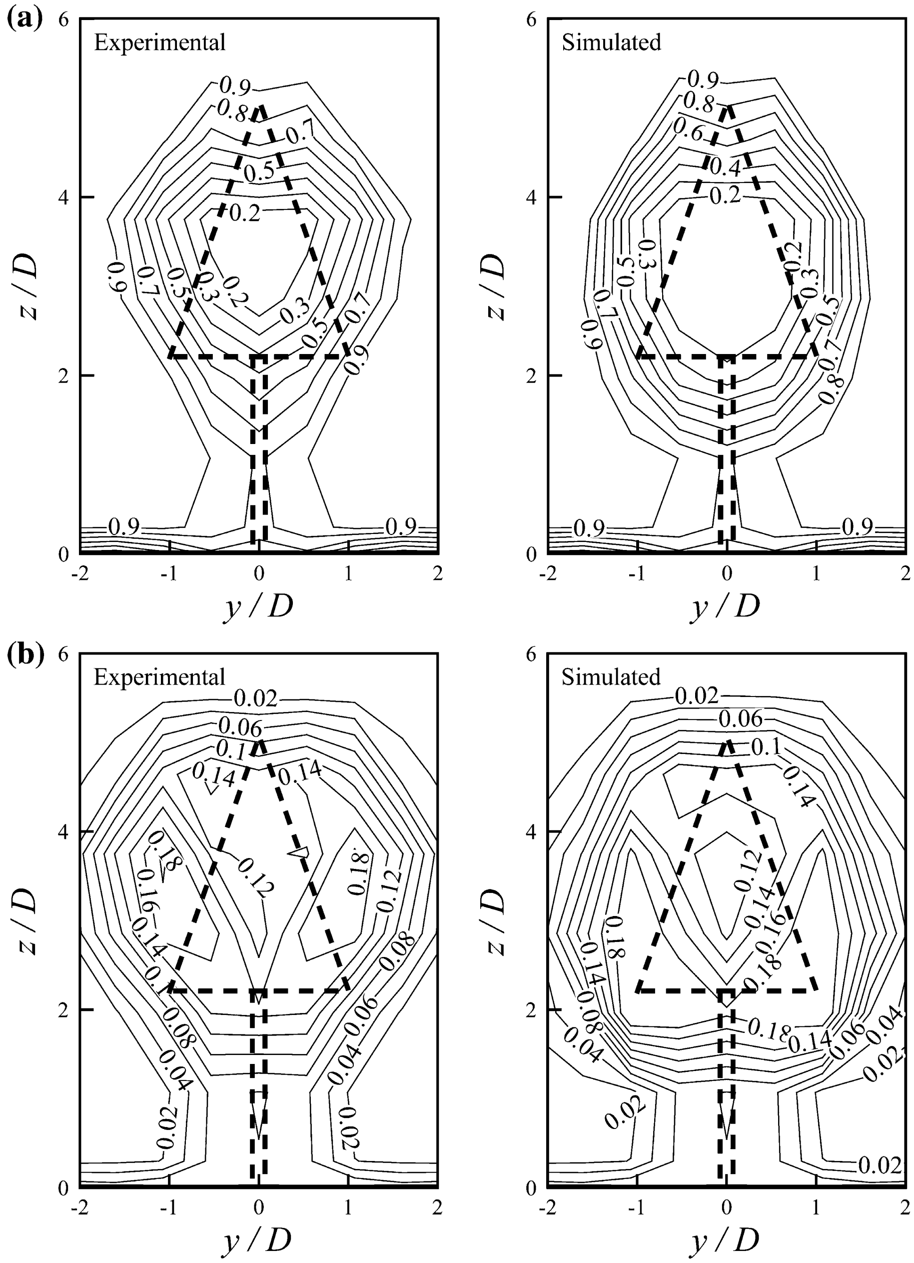

Figure 6. Comparison of mean and rms velocity profiles of an isolated tree. (a) Mean profiles ($\bar{u}/U_o$) and (b) rms profiles (u'/U_o).

Two vertical plates, with a separation distance of 0.8 m, were set at the side ends of the panels to produce 2-D flow patterns. The corresponding blockage ratio was less than 1%. A constant temperature anemometer (Dantec StreamLine 90N10) with a cross-film probe (55R61) was adopted to measure the downstream cross-sectional mean and root mean square (rms) velocity profiles at the center vertical plane. In the velocity measurements, the sampling rate was 100 Hz and the measurement period was 90 s. The measurement results were compared with those from the numerical computations.

5. Calibration of tree factor

As the factor of leaf surface area per unit volume ("a" value) proposed by Shaw and Schumann (1992) cannot be easily measured technically, a new parameter is proposed in the study as

$$C_{Da} = C_D a. \tag{17}$$

To investigate how C_{Da} varied with the conditions of trees, wind tunnel experiments were performed. In the experiments, rectangular panels (D = 0.28 m and B varies from 0.14–0.56 m) with various numbers of coniferous

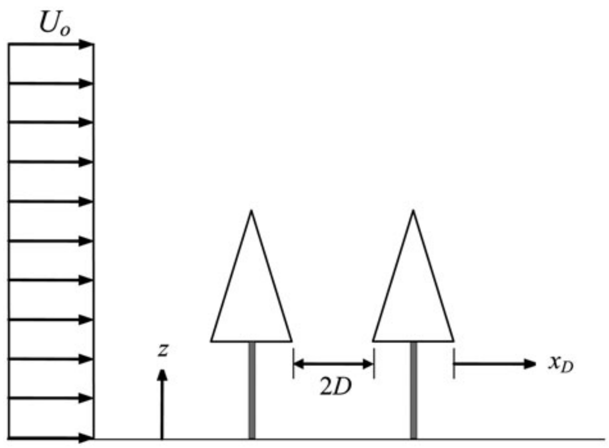

Figure 7. Schematic of flow past dual trees in a tandem arrangement.

leaf strings corresponding to different volumetric tree ratios (γ), defined as the tree volume per unit volume of space, were set in the test section and the downstream mean and rms velocity profiles were measured at several selected sections ($x_D = 4D$, $6D$, $8D$, and $10D$). On the other hand, a series of numerical simulations with a number of guessed C_{Da} values were also performed. By comparing with the measurement profiles corresponding to a prescribed thickness (B) and volumetric tree ratio (γ), the C_{Da} value that leads to the best agreement between the measurement and calculated profiles was then obtained. Figure 3 illustrates a typical example ($B = 0.5D$, $\gamma = 0.3\%$, $U_o = 10$ m/s, and $C_{Da} = 6.25$ m^{-1}) of the downstream mean and rms velocity profile comparisons.

Accordingly, Figure 4 depicts the contour plot of the resulting C_{Da} value in relation to the panel thickness (B) and the volumetric tree ratio (γ). The general tendency shows that an increase in the panel width or the volumetric tree ratio results in an increase in the C_{Da} value, except when B is less than about 0.15 m. In addition, the variation of C_{Da} appears mild, when B is greater than 0.56 m.

It is noted that the variation of the volumetric tree ratio (γ) generally covers the range of general engineering applications regarding coniferous trees. Due to spatial limitations of the wind tunnel tests, however, the resulting C_{Da} variation is valid for B less than 0.56 m.

6. Flow simulations

Based on the result in Figure 4, simulations were conducted further to examine the validity of the calibrated C_{Da} variations. In addition, parallel wind tunnel experiments were also carried out to measure the downstream velocity profiles for comparison. In all the 3-D flow computations, a uniform approaching flow was selected ($U_0 = 10$ m/s). To consider both the accuracy of the flow predictions and the efficiency of the numerical calculations, the vertical size of the computational domain was chosen as $14D$ ($D = 0.28$ m; see also Figures 5 and 7). In the longitudinal direction, the distances from the upstream and downstream end sections to the closest tree edges were, respectively, $10D$ and $20D$. On the other hand, the transverse distance from the domain sides to the tree edge was $10D$. Preliminary test results revealed that the relative error produced by this domain selection is no more than 3%.

6.1. *Uniform flow past an isolated coniferous tree with a conical shape*

Figure 5 depicts the schematic of the problem. In the computation, the tree body was divided into several layers, and the C_{Da} values associated with the grid cells in each layer were taken from the calibration contour plot (Figure 4) according to the corresponding horizontal thickness and volume ratio of the tree body. On the other hand, the main tree trunk, a circular cylinder with a diameter of $0.1D$ (0.05 m), was treated as a solid body in the flow simulation. The comparisons of normalized mean and rms velocity profiles at a typical downstream cross-section ($x_D = 6D$) are shown in Figure 6. The spatial correlation coefficients of the cross-sectional velocity variations between the experimental and calculated results are, respectively, 0.976 and 0.916, indicating a good prediction of the flow.

6.2. *Uniform flow past dual coniferous trees in a tandem arrangement*

An additional flow computation was conducted to simulate a uniform flow past dual coniferous trees in a tandem arrangement with an edge-to-edge distance of $2D$ (see Figure 7). The comparisons in Figure 8 show that the agreements between the measurement and the predicted results at a typical cross-section ($x_D = 6D$) appear also good. The spatial correlation coefficients of the comparisons are, respectively, 0.985 for the mean profiles and 0.901 for the rms profiles.

6.3. *Uniform flow past dual coniferous trees in a side-by-side arrangement*

A uniform flow past dual coniferous trees in a side-by-side arrangement with an edge-to-edge transverse distance of $0.5D$ was further simulated numerically. The comparisons in Figure 9 show that at a typical downstream cross-section ($x_D = 6D$), again, the predicted mean and fluctuating velocity profiles are predicted with acceptable accuracy (correlation coefficients are 0.939 and 0.912, respectively).

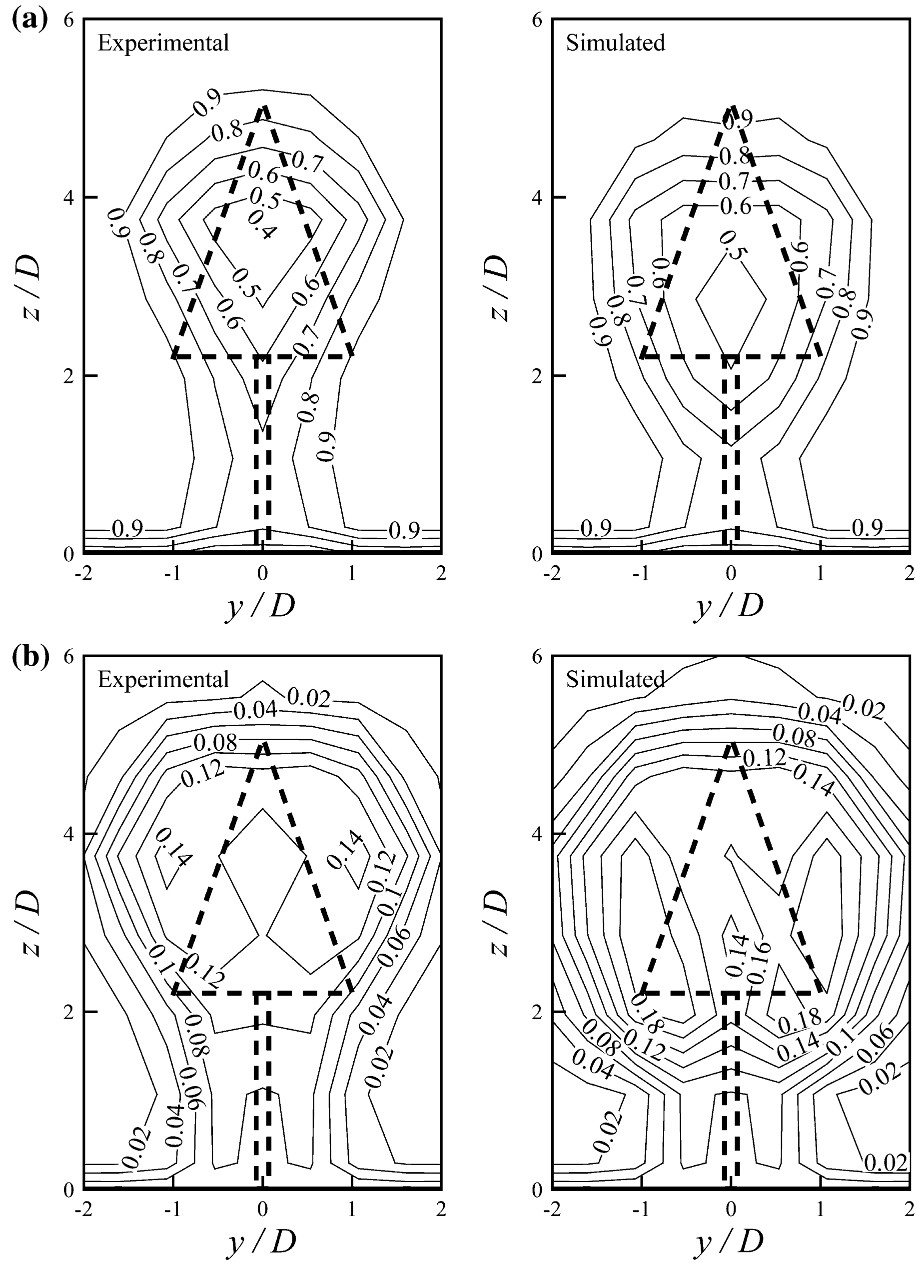

Figure 8. Comparison of mean and rms velocity profiles of dual trees in a tandem arrangement. (a) Mean profiles ($\bar{u}/U_o$) and (b) rms profiles (u'/U_o).

7. Discussion

Different from the analysis of flow past tree groups, this study attempted to investigate the effect of discrete trees in more detail, so as to provide extensive information regarding the local tree characteristics. Although the sway motion of trees due to wind action could affect the neighboring flow behavior (Flesch and Wilson 1999a, 1999b), it was not considered in the study to simplify the analysis.

To account for the effect due to the existence of a tree body, the form originally suggested by Shaw and Schumann (1992; see Equations (12) and (13)) reflects the retarding force in the flow due to the porous body as a result from the momentum deficit. Conceptually, this force leads to the integrated effect of the normalized drag, or drag coefficient (C_D), as well as the porosity of the tree leaves ("*a*" value in Equations 13). As mentioned previously, however, the factor "*a*", defined as the leaf surface area per unit volume, is hard to measure

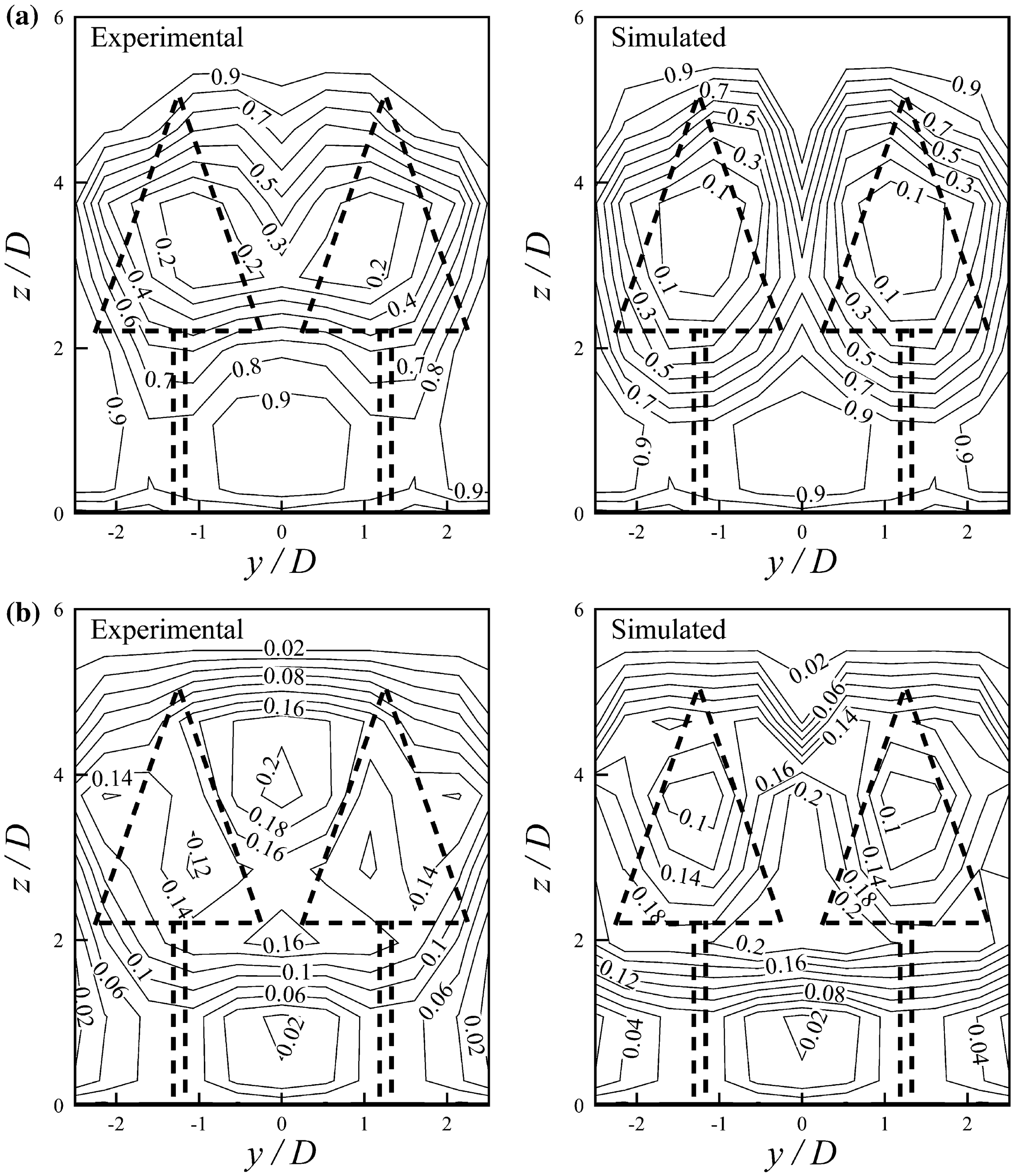

Figure 9. Comparison of mean and rms velocity profiles of dual trees in a side-by-side arrangement. (a) Mean profiles ($\bar{u}/U_o$) and (b) rms profiles (u'/U_o).

technically. Moreover, the drag is dependent on the local flow and is not yet determined. Therefore, this suggested form is not convenient to apply in the execution of the flow simulation in practice. Accordingly, a new concept that combines both C_D and "a" into a single parameter (C_{Da}) is proposed in this study. The basic idea is that, as the wind flow impinges on the tree body, the effect of the tree is mainly affected by the volume ratio of local leaves and twigs (γ) as well as the horizontal thickness (B), which are relatively easier to measure, and is compatible with the original concept by Shaw and Schumann (1992). After the variation of C_{Da} is obtained as the result of calibration (Figure 4), the application of this single parameter then allows for a handy way to solve the problem of a flow past porous trees numerically. As the numerical flow simulations in the three examples were successfully applied, it indicates that the C_{Da} variation (Figure 4) can be used to simulate flows past discrete trees with adequate accuracy.

The result in Figure 4 also indicates that as the thickness of the tree body is about $2D$ ($D = 0.28$ m), the variation of C_{Da} appears insignificant. Due to spatial considerations of the wind tunnel experiments, this study program is limited for a tree body thickness up to 0.56 m. Whether this tendency is valid beyond this range would require additional investigations in the future.

Finally, in all the flow simulations in the study, the Reynolds number in terms of the approaching flow speed (U_0) and the panel thickness (D) is about 3.83×10^5, which is generally considered large enough to achieve high Reynolds number invariance of the dimensionless flow results. In cases involving a much greater Reynolds number, however, the validity of the asymptotic invariance still needs extensive examination.

8. Conclusions

A method of identifying the tree factor was proposed. By comparing with the measurement results of the downstream velocity profiles of rectangular tree panels, the C_{Da} value associated with the thickness (B) and volume ratio (γ) of the tree body was calibrated numerically by a trial-and-error procedure. Accordingly, the variation of C_{Da} in relation to B and γ was presented. The variation of the volumetric tree ratio (γ) should cover the range of general engineering applications regarding coniferous trees. The validity range of B, however, is limited to 0.56 m. To simulate flows past a coniferous tree with a greater horizontal thickness in practice, an extended study is suggested in the future to find out the C_{Da} variation within a larger range of horizontal tree thickness.

Based on the calibrated contour plot of C_{Da}, simulations of uniform flows past an isolated tree, and dual trees in tandem and side-by-side arrangements were performed to examine the validity of the numerical method. The comparisons, in terms of the downstream mean and rms velocity profiles, indicated that the flows were well predicted.

Several conclusions are drawn as follows:

(1) A new parameter (C_{Da}) is proposed to characterize the effect of a porous tree body, which can be used for the simulation of flows past discrete coniferous trees.
(2) The general tendency shows that an increase in the thickness (B) or the volume ratio (γ) of the tree body results in an increase in the C_{Da} value, except when the thickness is less than about 0.15 m.
(3) When B exceeds 0.56 m, the variation of C_{Da} appears insignificant.
(4) As the sway motion of trees can be neglected, the calibrated variation of C_{Da} can be readily employed to simulate flows past discrete coniferous trees with adequate accuracy.

Nomenclature

a	leaf surface area per unit volume
B	horizontal thickness of tree body
C_S	Smagorinsky constant
C_D	drag coefficient
C_{Da}	tree parameter
c	speed of sound
D	transverse thickness of tree panel
$\boldsymbol{F}$	flux vector
$\boldsymbol{f_D}$	source term vector due to tree effect
G_m	mean quantity referred to the computational cell
K	bulk modulus of elasticity
$\boldsymbol{n}$	normal surface vector
p	pressure
t	time
U_o	approaching-flow speed
$\bar{u}$	mean wind speed in the longitudinal direction
u'	rms wind speed in the longitudinal direction
$\boldsymbol{V}$	velocity vector
x, y, z	spatial coordinates
x_D	downstream distance from tree edge
Δ	characteristic length of computational cell
γ	volumetric tree ratio
ρ	density
τ_{ij}	total shear stress term
$\forall$	volume of computational cell

Funding

The study was sponsored by National Science Council in Taiwan [grant number NSC 100-2221-E-005-068].

References

Boldes, U., J. Colman, and D. L. J. Maranon. 2001. "Field Study of the Flow Behind Single and Double Row Herbaceous Windbreaks." *Journal of Wind Engineering and Industrial Aerodynamics* 89 (7–8): 665–687. doi:10.1016/S0167-6105(01)00065-4.

Finnigan, J. 2000. "Turbulence in Plant Canopies." *Annual Review of Fluid Mechanics* 32 (1): 519–571. doi:10.1146/annurev.fluid.32.1.519.

Flesch, T. K., and J. D. Wilson. 1999a. "Wind and Remnant Tree Sway in Forest Cutblocks. I. Measured Winds in

Experimental Cutblocks." *Agricultural and Forest Meteorology* 93 (4): 229–242. doi:10.1016/S0168-1923(98)00112-9.

Flesch, T. K., and J. D. Wilson. 1999b. "Wind and Remnant Tree Sway in Forest Cutblocks. II. Relating Measured Tree Sway to Wind Statistics." *Agricultural and Forest Meteorology* 93 (4): 243–258. doi:10.1016/S0168-1923(98)00113-0.

Massman, W. 1987. "A Comparative Study of some Mathematical Models of the Mean Wind Structure and Aerodynamic Drag of Plant Canopies." *Boundary-Layer Meteorology* 40 (1–2): 179–197. doi:10.1007/BF00140075.

Mihailovic, D. T., B. Lalic, B. Rajkovic, and I. Arsenic. 1999. "A Roughness Sublayer Wind Profile above Non-uniform Surface." *Boundary-Layer Meteorology* 93 (3): 425–451. doi:10.1023/A:1002063405979.

Novak, M. D., J. S. Warland, A. L. Orchaansky, R. Ketler, and R. Green. 2000. "Wind Tunnel and Field Measurements of Turbulent Flow in Forests. Part I: Uniformly Thinned Stands." *Boundary-Layer Meteorology* 95 (3): 457–495. doi:10.1023/A:1002693625637.

Patton, E. G., and K. J. Davis. 2001. "Decaying Scalars Emitted by a Forest Canopy: A Numerical Study." *Boundary-Layer Meteorology* 100 (1): 91–129. doi:10.1023/A:1019223515444.

Raupach, M. R., R. A. Antonia, and S. Rajagopalan. 1991. "Rough-wall Turbulent Boundary Layers." *Applied Mechanics Reviews* 44 (1): 1–25. doi:10.1115/1.3119492.

Raupach, M. R., P. A. Coppin, and B. J. Legg. 1986. "Experiments on Scalar Dispersion within a Model Plant Canopy. Part I: The Turbulence Structure." *Boundary-Layer Meteorology* 35 (1–2): 21–52. doi:10.1007/BF00117300.

Shaw, R. H., and U. Schumann. 1992. "Large-eddy Simulation of Turbulent Flow Above and within a Forest." *Boundary-Layer Meteorology* 61 (1–2): 47–64. doi:10.1007/BF02033994.

Sladek, I., T. Bodnar, and K. Kozel. 2007. "On a Numerical Study of Atmospheric 2D and 3D-flows over a Complex Topography with Forest Including Pollution Dispersion." *Journal of Wind Engineering and Industrial Aerodynamics* 95 (9–11): 1424–1444. doi:10.1016/j.jweia.2007.02.024.

Smagorinsky, J. 1963. "General Circulation Experiments with Primitive Equations." *Monthly Weather Review* 91 (3): 99–164. doi:10.1175/1520-0493(1963)091<0099:GCEWTP>2.3.CO;2.

Song, C. C. S., and M. Yuan. 1988. "A Weakly Compressible Flow Model and Rapid Convergence Methods." *ASME Journal of Fluids Engineering* 110 (4): 441–455. doi:10.1115/1.3243575.

Su, H. B., R. H. Shaw, K. T. Pawu, C. H. Moeng, and P. P. Sullivan. 1998. "Turbulent Statistics of Neutrally Stratified Flow Within and above a Sparse Forest from Large-Eddy Simulation and Field Observations." *Boundary-Layer Meteorology* 88 (3): 363–397. doi:10.1023/A:1001108411184.

Watanabe, T. 2004. "Large Eddy Simulation of Coherent Turbulence Structures Associated with Scalar Ramps over Plant Canopies." *Boundary-Layer Meteorology* 112 (2): 307–341. doi:10.1023/B:BOUN.0000027912.84492.54.

Wilson, J. D., and T. K. Flesch. 1999. "Wind and Remnant Tree Sway in Forest Cutblocks. III. A Windflow Model to Diagnose Spatial Variation." *Agricultural and Forest Meteorology* 93 (4): 259–282. doi:10.1016/S0168-1923(98)00121-X.